

# Synthesis and Structural Peculiarities of 1,1-Dimethylhydrazine-Based Polyurethanes

Y. V. Savelyev,<sup>1</sup> V. Y. Veselov,<sup>1</sup> V. K. Kharitonova,<sup>1</sup> O. A. Savelyeva,<sup>1</sup> V. I. Shtompel,<sup>1</sup> A. I. Perekhrest,<sup>1</sup> T. V. Travinskaya,<sup>1</sup> A. Kanapitsas,<sup>2</sup> P. Pissis<sup>2</sup>

<sup>1</sup>*Institute of Macromolecular Chemistry, National Academy of Sciences of Ukraine, 02160 Kiev 160, Ukraine*

<sup>2</sup>*Department of Physics, National Technical University of Athens, Zografou Campus, 157 80 Athens, Greece*

Received 19 July 2007; accepted 10 October 2007

DOI 10.1002/app.28784

Published online 24 February 2009 in Wiley InterScience (www.interscience.wiley.com).

**ABSTRACT:** Novel polyurethanes (PUs) based on poly(oxytetramethylene glycol), 4,4'-methylenediphenyl diisocyanate, and 1,1-dimethylhydrazine (DMH) were prepared. Stoichiometric (1 : 1) and nonstoichiometric (2 : 1 to 20 : 1) prepolymer/DMH ratios were studied. The number-average molecular masses and possible structures of the obtained polymers were evaluated by potentiometric nonaqueous titration analysis of terminal groups, the Kjeldal method (the evaluation of the nitrogen atom content), the aminolysis method, viscosimetry, IR spectroscopy, rheology, and small-angle X-ray scattering. Only in the case of the stoichiometric (1 : 1) ratio

was a low-molecular-mass PU with a linear structure formed, whereas for all studied nonstoichiometric ratios, PUs with branched structures were formed. The level of hard and flexible block segregation increased with the increase in the prepolymer/DMH ratio. Dielectric results for the dynamic glass transition and water sorption measurements provided additional support to the structural studies. © 2009 Wiley Periodicals, Inc. *J Appl Polym Sci* 112: 2732–2740, 2009

**Key words:** polyurethanes; structure-property relations; synthesis

## INTRODUCTION

Hydrazine organic derivatives are of great importance in hydrazine chemistry because of their high reactivity. Previous attempts at applying 1,1-dimethylhydrazine (DMH) in macromolecular chemistry have been mainly directed toward its use for polymer modification.<sup>1</sup> The high reactivity of the tertiary nitrogen atom of DMH leads to the formation of hydrazinium compounds. Thus, for quaternization of the tertiary nitrogen atom, the nitrogen atom of the amine group may react only under conditions of steric hindrance.<sup>2,3</sup> That is why the use of hydrazine derivatives in the processes of polyurethane (PU) formation is problematic.

As a rule, PUs are obtained by a two-step process: the formation of a prepolymer (PP) with terminal NCO groups through the reaction of poly(ether ester)s with diisocyanates and the extension of the PP with bifunctional compounds containing active H atoms [chain extender (CE)]. With an equimolar ratio of PP to CE, linear PU is formed, unlike with nonequimolar ratios, with which linear PU cannot be generated.<sup>4</sup> However, the treatment of PP with DMH at various nonequimolar ratios does not lead

to crosslinking, and PUs soluble in organic solvents are formed.<sup>5</sup> To explain these results, a model reaction of the formation of urethane between DMH and phenylisocyanate (PhIC) has been studied.<sup>6</sup> This reaction should result in the formation of 1,1-dimethyl-4-phenylsemicarbazide [Fig. 1(I)] in accordance with classical conceptions of the interactions of isocyanates with hydrazides (or amines). However, an investigation of the chemical structure of the reaction products (at various reagent ratios) by IR and NMR spectroscopy showed the fallacy of this assumption.<sup>6</sup> The reaction of DMH and PhIC was not completed with 1,1-dimethyl-4-phenylsemicarbazide as the main product, and compounds of biuret-like structures [Fig. 1(II,III)] were formed. Only in the case of a considerable excess of DMH with respect to PhIC was 1,1-dimethyl-4-phenylsemicarbazide [Fig. 1(I)] obtained as the main product.<sup>6</sup>

The objective of this work was to study the chemical aspects of DMH-based PU formation with different reagent ratios and to characterize their structure and performance with a complex of independent chemical and physical methods.

## EXPERIMENTAL

### Materials

Industrial DMH was distilled under an alkali in dry N<sub>2</sub>, and poly(oxytetramethylene glycol) with a

Correspondence to: Y. V. Savelyev (yusav@i.kiev.ua).

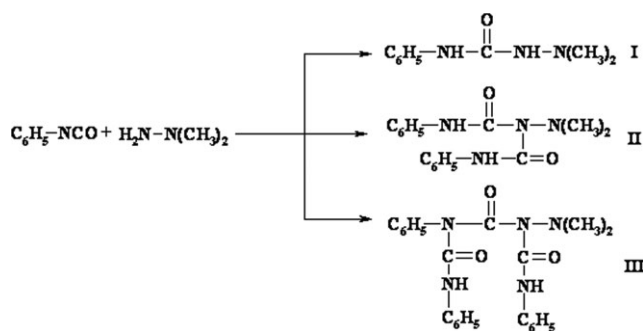


**Figure 1** Scheme of the model compounds obtained through the reaction of DMH and PhIC.

molecular weight of 1000 was dried *in vacuo* at 80°C. 4,4'-Methylene bis(phenyl isocyanate) was distilled *in vacuo*, and *N,N'*-dimethylformamide (DMF) and diethylamine (DEA) were purified with standard methods.

### Synthesis

PP was obtained through the reaction of poly(oxytetramethylene glycol) and 4,4'-methylene bis(phenyl isocyanate) at [NCO]/[OH] = 2. DMH was added to a PP solution in DMF at the ambient temperature. Then, the PP/DMH mixture was blended at 60–80°C until the full exhaustion of NCO groups (IR control, 2280 cm<sup>-1</sup>). Solutions of the PUs in DMF were degassed *in vacuo* and cast onto a glass plate. Films of the PUs were formed at the ambient temperature and dried at 60°C *in vacuo*. The compositions and properties of the obtained PUs are presented in Table I. Stoichiometric (1 : 1) and nonstoichiometric (2 : 1 to 20 : 1) PP/DMH ratios were studied (Table I).

The aminolysis reaction was used to indicate the presence of biuret and allophanate fragments in the PU. A 0.3 M solution of DEA in DMF (in a triple quantity with respect to the theoretical amounts of biuret and allophanate fragments) was added to the PU solution in DMF, and the mixture was stirred and stored at 25–30°C for 2 h. An excess of DEA was eliminated *in vacuo* at the ambient temperature.

DEA-based PUs were obtained for comparison under the same conditions as DMH-based PUs at a PP-to-DEA ratio of 1–20 : 1.

### Methods

The kinetics of the PU formation reaction with various catalysts {triethylamine (TEA), tin dibutyl dilaurate (TDBDL), and tin acetyl acetonate [Sn(AcAc)<sub>2</sub>Cl<sub>2</sub>]} were studied with IR spectroscopy. The change in the NCO group concentration was controlled by the relative intensity of the adsorption band of stretching vibrations of NCO groups (2270 cm<sup>-1</sup>), with the intensity of the methylene band at 2860 cm<sup>-1</sup> used as the internal reference. IR spectra were recorded with a UR-20 spectrometer in the range of 400–4000 cm<sup>-1</sup>.

The contents and numbers of the associated *N,N*-dimethylhydrazine groups, *N*-substituted amide groups (>NCO—), and *N*-amide and attached hydrazine groups in the polymer chain were determined by potentiometric nonaqueous titration<sup>7</sup> with an Ionometr I-160 (Avtomatica, Minsk, Belarus) with chlor-argentum, glass and platinum electrodes, a PE-6110 magnetic stirrer (Ekros, Warsaw, Poland), and a computer for graphic interpretation and data recording.

To evaluate the number-average molecular weights (*M<sub>n</sub>*'s) of the polymers, the analysis of terminal groups was applied. The *M<sub>n</sub>* values were calculated according to

$$M_n = 1000 \times (R/100) \times m/M_{\text{HClO}_4} \times V$$

where *R* is the content of the solid residue (%), *m* is the weight of the polymer solution taken for analysis (g), *M<sub>HClO<sub>4</sub></sub>*

is the solution molarity of HClO<sub>4</sub> (mol/L), and *V* is the volume of the titrant that was expended for the end point of the equivalent (mL). The content and number of the associated *N,N*-dimethylhydrazine groups were determined by potentiometric titration in an acetic solution of chloric acid in a medium of iced acetic acid

**TABLE I**  
Compositions and Some Properties of the Prepared PUs: [η], Density, Strength, and Relative Elongation at Break

Polymer	PP/DMH	[NCO]/[NH <sub>2</sub> ]	[η]	Density (g/cm <sup>3</sup> )	Strength (MPa)	Relative elongation at break (%)
G1/1	1 : 1	2	0.34	1.0866	7.5	180
G2/1	2 : 1	4	0.72	1.1235	24.5	630
G3/1	3 : 1	6	0.68	1.1227	24.1	650
G4/1	4 : 1	8	0.56	1.1157	23.7	700
G5/1	5 : 1	10	0.57	1.1126	23.3	725
G6/1	6 : 1	12	0.55	1.1124	23.1	767
G7/1	7 : 1	14	0.54	1.1119	22.8	773
G8/1	8 : 1	16	0.49	1.1115	22.5	781
G9/1	9 : 1	18	0.50	1.1112	22.4	793
G10/1	10 : 1	20	0.51	1.1111	22.2	801
G20/1	20 : 1	40	0.66	1.1017	26.1	958

The definition of the content and number of *N*-substituted amide groups ( $>\text{NCO}-$ ) ( $X_{>\text{NCO}-}$ ) was carried out according to potentiometric titration in a methanol solution of KOH in a medium of mixed dioxane and acetonitrile (1 : 2).

The number of *N*-amide and attached hydrazine groups was determined by titration and calculated with the obtained values of  $M_n$  and  $X_{>\text{NCO}-}$ .

The amount of nitrogen atoms in the macrochain was evaluated by the Kjeldal method<sup>8</sup> with a Shott titrator (Mainz, Germany).

The intrinsic viscosity ( $[\eta]$ ) was determined with an Ubbelohde viscosimeter (Khimlabsteklo, Klin, Russia) in a DMF-polymer solution. The dynamic viscosity was measured with a Rheotest-2 rotational viscosimeter (VEB MLW Prufgerate-werk, Medingen, Germany) with a cylindrical measuring device at room temperature.

The structure of DMH-based PUs and PUs after aminolysis was controlled with a Tensor-37 Fourier transform infrared (FTIR) spectrometer (Bruker, Ettlingen, Germany) in the range of 400–4000  $\text{cm}^{-1}$ .

A KRM-type diffractometer (Nauchpribor, Orel, Russia) (Ni-filtered copper radiation,  $K\alpha = 0.154$  nm) was used for small-angle X-ray scattering (SAXS) measurements with scattering angles of 0.1–3° at the sample-to-detector distance of 27 cm. The scattering curves were normalized by the scattering volume and corrected for the absorption of X-rays by the sample.<sup>9</sup> The Bragg period ( $D$ ; the average distance of the proximate next domains in a dimensional macrolattice) was calculated with the Bragg equation.<sup>10</sup> The degree of microphase segregation ( $\alpha_{\text{seg}}$ ) of flexible and hard blocks in PU was calculated according to Bonart et al.<sup>11</sup>

Mechanical properties were tested with an upgraded RM-30-1 test machine (constructed at Ivanovo Measure-Works, Russia).

The dynamic glass transition of PU was investigated by dielectric relaxation spectroscopy (DRS). A Schlumberger FRA SI 1260 frequency response analyzer (Farnborough, UK), supplemented by a buffer amplifier of variable gain (Chelsea Dielectric Interface, Holt Heath, UK) and a Hewlett-Packard 4284A (Palo Alto, CA) precision LCR meter, was used in combination with the Novocontrol Quatro (Hundsangen, Germany) cryosystem.<sup>12</sup> Equilibrium water sorption isotherms were measured at 25°C. The water content (grams of water per gram of dry sample) was determined by weighing (A200S analytical balance, Sartorius, Goettingen, Germany).<sup>13</sup>

## RESULTS AND DISCUSSION

The compositions and properties of the synthesized PUs are presented in Table I. At the PP/DMH stoichiometric ratio of 1 : 1, a linear low-molecular-

weight polymer was formed (Table I, sample G1/1). At nonstoichiometric ratios of PP/DMH ranging from 2 : 1 to 20 : 1 (Table I, samples G2/1–G20/1), film-forming polymers with high mechanical indices, soluble in organic solvents, were obtained.

The content of NCO groups was found to drastically decrease to 20–22% for all polymer specimens without a catalyst. For G2/1 with  $\text{Sn}(\text{AcAc})_2\text{Cl}_2$  as a catalyst, the content of NCO groups decreased to 0% in 20 min at room temperature. When TDBDL was used, the content of NCO groups decreased to 0% in 60 min at room temperature and in 30 min at 60°C. With TEA as the catalyst, the content of NCO groups decreased to 0% in 60 min at room temperature, to 2.2% in 10 min at 60°C, and to 0% in 10 min at 80°C. According to their activity in the reaction of urethane formation, the catalysts can be arranged as follows:  $\text{Sn}(\text{AcAc})_2\text{Cl}_2 > \text{TDBDL} > \text{TEA}$ . It is known<sup>14</sup> that the use of a hydrazine derivative as a CE and metal acetyl acetonate as a catalyst in the reaction of PU formation results in the formation of an intermediate catalyst-dihydrazide complex, which is responsible for the acceleration of the reaction. Taking into account that metal  $\beta$ -diketonates [e.g.,  $\text{Sn}(\text{AcAc})_2\text{Cl}_2$ ] play a catalytic role in PU formation reactions between tin organic compounds and tertiary amines,<sup>4,15</sup> we find that the highest activity of  $\text{Sn}(\text{AcAc})_2\text{Cl}_2$  cannot be explained only by the formation of the  $\text{Sn}(\text{AcAc})_2\text{Cl}_2$ -DMH complex. Using the complex approach based on the determination of (1) the number of amide groups and attached hydrazine groups by potentiometric titration and (2) the content of nitrogen atoms by the Kjeldal method, we can evaluate the  $M_n$  values and predetermine the possible structures of the obtained macromolecules (Table II). Thus, oligomers and low-molecular-mass linear polymers are formed only at PP/DMH ratios of 1 : 1 and 2 : 1 [catalytic reaction; Fig. 2(A)]. In all other cases, polymers of branched structures (comb-like) are formed [Fig. 2(B,C)] because of the formation of biuret and allophanate bonds.

It is known<sup>16</sup> that phosphoric acid prevents biuret bond formation. The molecular masses of the final products decreased when phosphoric acid was introduced into the reactive system (Table II, sample G2/1<sup>2</sup>). This result provides additional support for the formation of biuret bonds at PP/DMH ratios higher than 1 : 1. Macromolecular branching affects the rheological characteristics of a polymer. As a rule, the branching of a macromolecule reduces the polymer viscosity only when the length of the side chains is not comparable with the length of the main chain and the macromolecule does not assume the star configuration.<sup>4</sup>

This effect of the reduction of  $[\eta]$  on the studied polymers is presented in Table I.  $[\eta]$  decreased as the PP/DMH ratio increased (from 2 : 1 to 10 : 1); at

TABLE II  
Structures and Molecular Masses from the Structures of the Prepared PUs

Polymer sample	$M_n$ based on potentiometric data	Amount of DMH end groups	Amount of <i>N</i> -amide terminal groups	Amount of N atoms	Possible structures	$M_n$ from the structure
G1/1	3,446	1	1	10	(A) <sub>3</sub>	4,200
G2/1	7,563	1	1	15	(B) <sub>2</sub>	7,150
G2/1 <sup>a</sup>	3,461	1	1	10	(A) <sub>3</sub>	4,200
G2/1 <sup>b</sup>	5,790	1	1	17	(B) <sub>2</sub>	5,800
G5/1	9,808	1	5	24	(C) <sub>2</sub>	9,050
G10/1	23,981	1	5	52	(C) <sub>5</sub>	22,400
G20/1	35,834	2	17	96	(C) <sub>9</sub>	40,250

<sup>a</sup> In the presence of TDBDL as a catalyst.

<sup>b</sup> In the presence of H<sub>3</sub>PO<sub>4</sub>.

the same time, the molecular masses increased (Table II). The opposite dependence was observed for the reference polymers based on DEA:  $[\eta]$  of the PU solutions increased as the PP-to-DEA ratio increased (Table III). These results may be explained by the formation of branched structures. The increase in  $[\eta]$  for PP/DMH ratios higher than 10 : 1, particularly for the sample G20/1, may indicate the formation of branched macromolecules with side branches comparable in length to the main chain.

According to dynamic viscosity data, the behavior of PU is typical for polymeric systems: the viscosity coefficient decreases as the shear rate increases. The viscosity anomaly [Fig. 3(1bc)] and the drastic reduction of the viscosity with the shear stress ( $\tau$ ) increase [Fig. 4(1)] are most obvious for G2/1. At very low [Fig. 3(1ab)] and very high [Fig. 3(1cd)] stresses and shear rates, we observed Newtonian flow for samples G2/1–G20/1. For the comparative characteristic of PU, we used the effective viscosity ( $\eta_{ef}$ ), which corresponded to the set value of  $\tau$ . Thus, at a low  $\tau$  value (0.2 N/m<sup>2</sup>),  $\eta_{ef}$  for both G2/1 and G10/1 was 0.75 Pa s. As  $\tau$  rose to 0.3 N/m<sup>2</sup>, the viscosity of G2/1 dropped roughly and attained a minimal value 5 times lower than the initial one. With the completely destroyed structure and high  $\tau$  values ( $\tau = 2.6$  N/m<sup>2</sup>),  $\eta_{ef}$  for G2/1 and G10/1 was 0.210 and

0.375 Pa s, respectively. In other words, the viscosity of the completely destroyed structure descended in the order of G20/1 > G10/1 > ... G2/1. The transition from Newtonian flow to unsteady flow occurred in a narrow area of stresses, and the range of the viscosity anomaly was rather narrow. One of the reasons for the viscosity anomaly of the studied systems is thixotropy.<sup>17</sup> This phenomenon can be explained by changes in the supramolecular structure and macromolecular shape under the influence of stress and their recovery after stress elimination. As mentioned previously, the viscosity of polymers also depends on the branchness of the macromolecules. The branchness reduces the viscosity (as shown for the studied systems; see Table I). If the length of the side branches is comparable to the length of the main chain, a reduction of the viscosity is not observed (at PP/DMH > 10). The reduction of the PU viscosity at a nonstoichiometric PP/DMH ratio may marginally testify to the formation of branched polymers.

The capability of DMH to generate hydrazinium cations<sup>2</sup> suggests that the reaction of PU formation with DMH participation proceeds via the generation of ionic reactive centers.<sup>18</sup> The fact that tin acetyl acetonate dichloride (which can stimulate cation formation) shows the highest activity in comparison

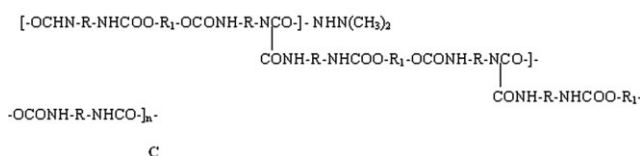
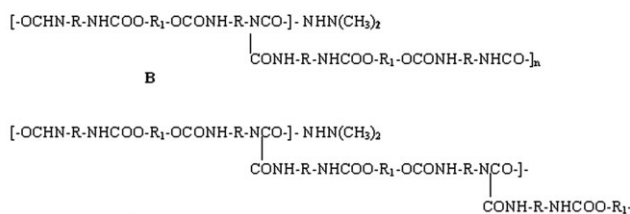
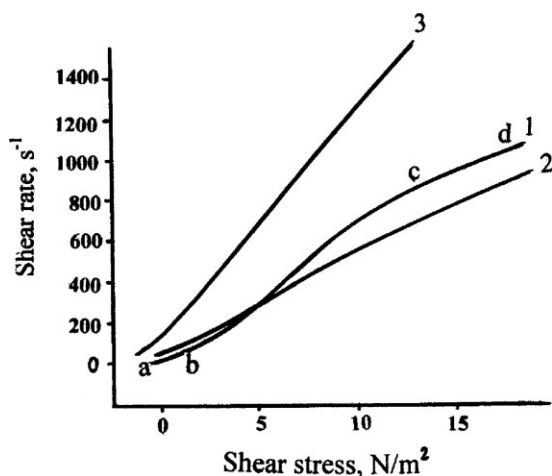


Figure 2 PU macromolecular structures: (A) linear and (B, C) branched.

TABLE III  
 $[\eta]$  of the Polymers Versus the Component Ratio

DMH-based PU	$[\eta]$	PU for comparison	$[\eta]$
1 : 1 PP/DMH	0.34	1 : 1 PP/DEA	0.18
2 : 1 PP/DMH	0.72	2 : 1 PP/DEA	0.35
3 : 1 PP/DMH	0.68	—	—
4 : 1 PP/DMH	0.56	4 : 1 PP/DEA	0.43
5 : 1 PP/DMH	0.57	5 : 1 PP/DEA	0.48
6 : 1 PP/DMH	0.55	—	—
7 : 1 PP/DMH	0.54	—	—
8 : 1 PP/DMH	0.49	—	—
9 : 1 PP/DMH	0.50	—	—
10 : 1 PP/DMH	0.51	10 : 1 PP/DEA	0.56
20 : 1 PP/DMH	0.66	20 : 1 PP/DEA	0.61



**Figure 3** Rheological curves of the flow of the polymer samples: (1) G10/1, (2) G20/1, and (3) G2/1.

with TEA and TDBDL, as described previously, confirms this hypothesis. The process of PU formation in the presence of hydrochloric acid provides the main evidence that the reaction proceeds via the generation of ionic reactive centers: the addition of the acid (DMH/HCl = 1 : 1) completes the reaction (100% NCO conversion) in 70 min at room temperature and in 15 min at 60°C, whereas under ordinary conditions at room temperature, the reaction extends over 120–180 min.

Reactions of the biuret formation of urea with isocyanates without a catalyst are possible only at 100°C and higher.<sup>4</sup> The creation of allophanates, if not catalyzed, proceeds at sufficient rates only at 120–140°C. However, an analysis of the structures of our PUs obtained at 60 and 80°C without catalysts

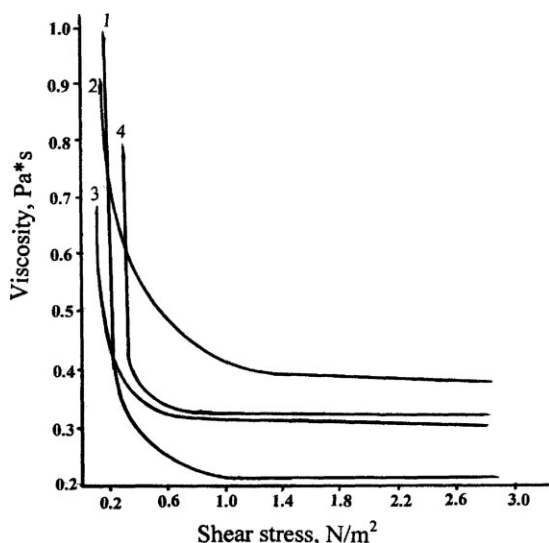


**Figure 4** Dependence of the dynamic viscosity of the polymer samples on  $\tau$ : (1) G2/1, (2) G10/1, (3) G4/1, and (4) G6/1.

**TABLE IV**  
Dependence of the Structure of Sample G2/1 on the Reaction Temperature

Polymer specimen (temperature)	Amount of N atoms	Amount of DMH end groups	Amount of <i>N</i> -amide terminal groups	$M_n$ from the structure
G2/1(60°C)	10	1	1	3410
G2/1(80°C)	17	1	1	6850

(Table IV) indicates the formation of branched PUs at temperatures lower than those typical for the formation of allophanate and biuret structures.

The IR spectra of the DMH-based polymers (Fig. 5) show all characteristic adsorption bands of PU-ureas: CH<sub>2</sub> groups (2857 and 2941 cm<sup>-1</sup>), COC groups (1112 cm<sup>-1</sup>), free CO groups of a urethane fragment (1730 cm<sup>-1</sup>), associated CO groups of a urethane fragment (1710 cm<sup>-1</sup>), CO groups of urea and/or biuret/allophanate fragments (1650 and 1670 cm<sup>-1</sup>), and NH groups (ca. 3300 cm<sup>-1</sup>). A detailed comparative analysis of the IR spectra of PUs [G1/2 ([NCO]/[NH<sub>2</sub>] = 1), G2/1 ([NCO]/[NH<sub>2</sub>] = 4) and G20/1 ([NCO]/[NH<sub>2</sub>] = 40) with different NCO/NH<sub>2</sub> ratios was carried out. The distinction of these polymers lies in the different contents of DMH and biuret/allophanate fragments and, as result, in the chain structure (linear and branched). The essential distinction of the G2/1 spectrum [Fig. 5(2)] lies in the existence of a clearly visible intensive shoulder with a maximum at 1670 cm<sup>-1</sup>, which can be designated as the biuret-group band.<sup>19</sup> The identification of biuret and allophanate fragments in IR spectra in some cases is difficult because of the overlaying of the absorption of other functional groups of PU.<sup>20</sup> In this case, the polymer G1/2 [Fig. 5(1)] can be used

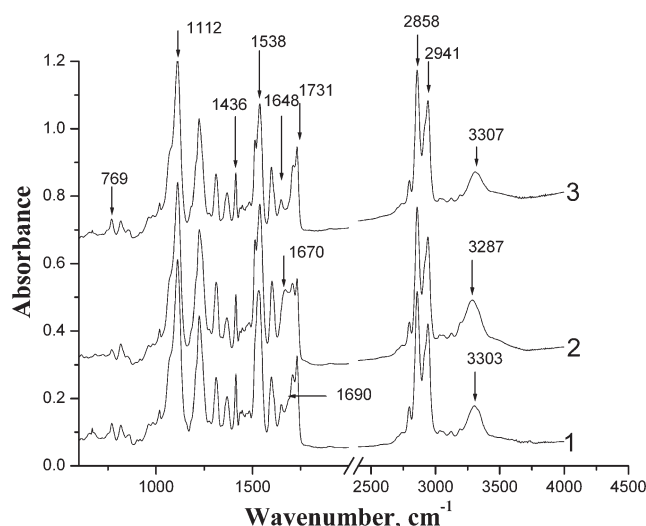


**Figure 5** FTIR spectra of the PUs: (1) G1/2, (2) G2/1, and (3) G20/1.

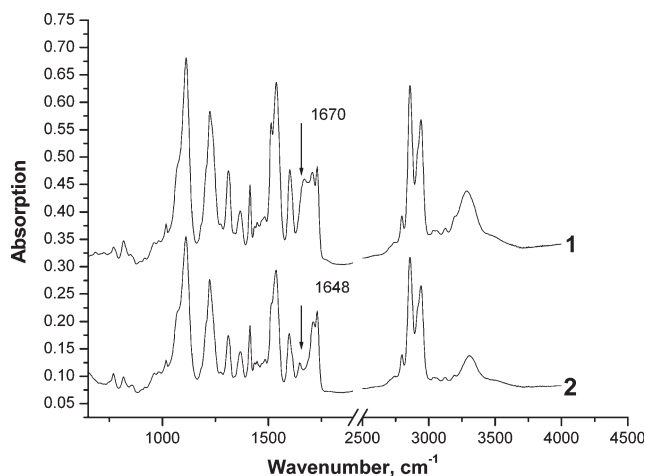
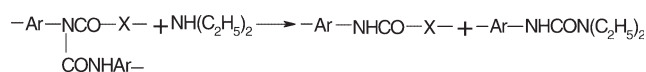


**Figure 6** FTIR spectra of (1) G2/1 and (2) G2/1 after treatment by DEA.

as a reference because the chance of biuret fragment formation at  $[\text{NCO}]/[\text{NH}_2] = 1$  is very low. Thus, the weak peak at  $1650\text{ cm}^{-1}$  as well as the shoulder at  $1690\text{ cm}^{-1}$  [Fig. 5(1)] can be attributed to CO groups of various association levels in the  $-\text{NH}-\text{CO}-\text{NH}-\text{N}(\text{CH}_3)_2$  fragment. In transit from G1/2 to G20/1 [Fig. 5(1.3)], the molar content of such fragments decreases by a factor of nearly 14; however, the relative intensity of the peak at  $1648\text{ cm}^{-1}$  increases. This can be explained by the overlapping of the absorption of valence vibrations of CO groups of the  $-\text{NH}-\text{CO}-\text{NH}-\text{N}(\text{CH}_3)_2$  fragment and CO groups of the allophanate/biuret fragments. The comparative analysis of the IR spectra of PUs G2/1 (curve 2) and G20/1 (curve 3), as well as the previous discussion, allows us to conclude that the content of biuret fragments in G2/1 is essentially higher than that in G20/1 and confirms the presented structures: B for sample G2/1 and C for sample G20/1 (Fig. 2). This is due to the effect of a 7 times greater molar content of urea fragments in G2/1 before the reaction of biuret formation in comparison with G20/1. The activity of urea groups in reactions with isocyanate groups greatly exceeds the activity of urethane groups.<sup>4</sup> According to the IR spectrum of G2/1 [Fig. 5(2)], either the content of allophanate fragments in this case is very low, or they are fully absent.

We have checked our assumption regarding the presence of allophanate and biuret fragments (responsible for the chain structure) in DMH-based PUs using the reaction of aminolysis<sup>20</sup> with DEA:



As a result of this reaction, *N,N*-diethyl-*N*-aryl-urea is formed with the characteristic band at  $1650\text{ cm}^{-1}$  for PUs based on aromatic diisocyanate.<sup>20</sup> In the

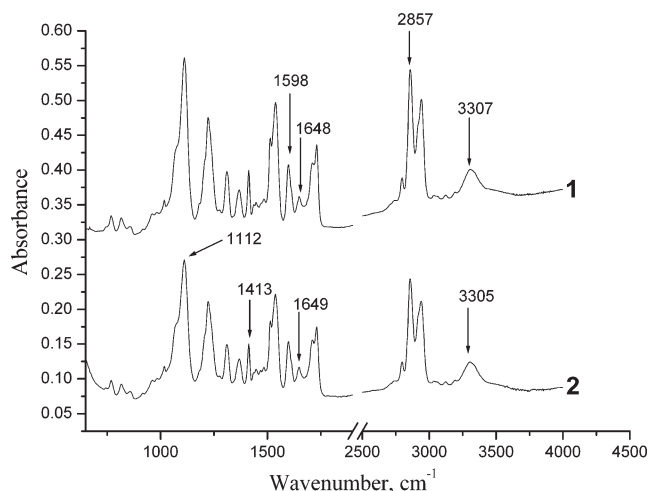


**Figure 7** FTIR spectra of (1) G20/1 and (2) G20/1 after treatment by DEA.

case of DMH-based PUs, the correct quantity calculations are complicated because of the complex absorption in the region of  $1650\text{ cm}^{-1}$  of DMH urea and other polar fragments. However, the essential changes can be observed in the IR spectrum of G2/1 after the aminolysis (Fig. 6). The exposure of the G2/1 sample in the DEA solution [Fig. 6(2)] led to the absence of the well-pronounced shoulder at  $1670\text{ cm}^{-1}$  and the appearance of the peak at  $1648\text{ cm}^{-1}$ . This testifies to a large number of biuret fragments (exposed to aminolysis) in the sample G2/1, which caused the shoulder at  $1670\text{ cm}^{-1}$  [Fig. 6(1)]. The aminolysis reaction of G20/1 did not generate essential changes in the IR spectrum (Fig. 7), except for the increase in the relative intensity of the  $1650\text{-cm}^{-1}$  band (Table V). The following groups were used as

**TABLE V**  
Relative Intensities of the  $1648\text{-cm}^{-1}$  Absorption Band in the Linear and Branched PUs

Sample	$I^{1112\text{ a}}$	$I^{1600\text{ b}}$	$I^{2857\text{ c}}$	$I^{1413\text{ d}}$
G20/1	0.07447	0.23729	0.09032	0.27132
G20/1 + DEA	0.10270	0.30159	0.11875	0.34545
(G20/1 + DEA)/ G20/1 <sup>e</sup>	1.4	1.3	1.3	1.3
G1/2	0.08290	0.27586	0.09816	0.27586
G1/2 + DEA	0.08671	0.27777	0.10043	0.28301
(G1/2 + DEA)/ G1/2 <sup>e</sup>	1.0	1.0	1.0	1.0

<sup>a</sup> Relative intensity of the  $1648\text{-cm}^{-1}$  peak when the intensity of the  $1112\text{-cm}^{-1}$  band was used as the internal standard:  $I^{1648} = D^{1648}/D^{1112}$ , where  $D^{1648}$  is the intensity of the absorbance of the  $1648\text{-cm}^{-1}$  peak and  $D^{1112}$  is the intensity of the absorbance of the  $1112\text{-cm}^{-1}$  peak.

<sup>b,c,d</sup> Calculated similar to <sup>a</sup>.

<sup>e</sup> Ratio of the relative intensities of the  $1648\text{-cm}^{-1}$  peaks after aminolysis (G20/1 + DEA and G1/2 + DEA) and before aminolysis (G20/1 and G1/2).

internal standards for the intensities of absorption bands: 1112 ( $\nu_{\text{COC}}$ ), 1600 ( $\nu_{\text{Ar}}$ ), 2857 ( $\nu_{\text{CH}}$ ), and 1413  $\text{cm}^{-1}$  ( $\delta_{\text{CH}}$ ). For the confirmation of the accuracy of the analogue calculations, detailed calculations for polymer G1/2 (which did not contain biuret and allophanate fragments) before and after its treatment with a DEA solution were performed. (Table V). The relative intensity of the band at 1650  $\text{cm}^{-1}$  did not change after the treatment in the DEA solution because of the lack of allophanate and biuret fragments. These data indicate the presence in G20/1 of biuret and allophanate fragments, which interacted with DEA with the appearance of aryl-urea fragments, leading to the increase in the peak (1650- $\text{cm}^{-1}$ ) intensity. Thus, the increase in the PP/DMH ratio to 2 led to biuret fragment formation, whereas the further increase in the excess of PP/DMH (PP/DMH = 20) led to allophanate fragment formation in the absence of catalysts and at relatively low temperatures (not higher than 80°C).

Now we discuss the results of SAXS measurements. Although the sample G1/1 (PP/DMH = 1 : 1) was characterized by structural heterogeneity (Fig. 8), the spatial position of the areas of heterogeneity (hard and flexible domains) of this PU demonstrated a weak periodicity with the value of  $D \approx 21$  nm. The changes in the scattering intensity in the angular area of  $2\Theta = 5\text{--}60^\circ$  and the conspicuous kink [at an angle of the interferential maximum ( $2\Theta_{\text{max}}$ ) of ca. 25°] confirmed the aforementioned observation and explained the presence of a weak interferential maximum on the scattering profile [Fig. 8(4)]. At the same time, the increase in the PP/DMH ratio (sample G2/1) enhanced the partial decrease in  $\alpha_{\text{seg}}$  of the flexible and hard PU blocks

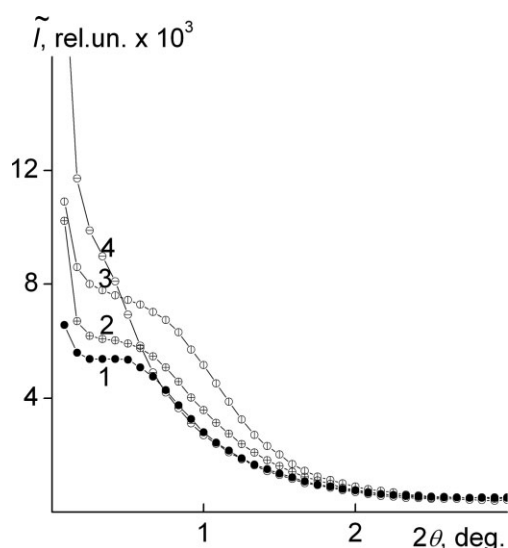


**Figure 8** SAXS patterns of some prepared PUs: (1) G2/1, (2) G5/1, (3) G10/1, and (4) G1/1.

**TABLE VI**  
SAXS Data for Selected PUs:  $2\Theta_{\text{max}}$ ,  $D$ , and  $\alpha_{\text{seg}}$

Polymer	$2\Theta_{\text{max}}$ (°)	$D$ (nm)	$\alpha_{\text{seg}}$
G1/1	25	21	0.23
G2/1	30	17.5	0.17
G5/1	32	16	0.29
G10/1	42	12.5	0.54

(Table VI) and, contrary to our representations, resulted in an increase of the regularity in a spatial layout of hard and flexible domains and in a decrease in  $D$  ( $D \approx 17.5$  nm) in comparison with those for the initial sample G1/1. The reduction of the DMH content by 5 and 10 times (samples G5/1 and G10/1) promoted an increase of  $\alpha_{\text{seg}}$  and a further decrease of  $D$  between the proximate centers of domains with equal electronic density (Table VI) in comparison with G1/1 and G2/1 polymers. Observed changes in the domain structure of hard blocks of PU with a consecutive reduction of the molar part of DMH indicated the diverse nature of the factors that initiated the structure formation processes in polymer samples G1/1, G2/1, G5/1, and G10/1. The rather low value of  $\alpha_{\text{seg}}$  and the weak dimensional ordering of hard and flexible domains in the G1/1 volume in comparison with the other polymers can be explained by the presence of  $\text{CH}_3$  groups, which created steric hindrances for the realization of short-range intermolecular hydrogen bonds with the participation of polar groups of hard blocks, along with the different structure of the macrochain.<sup>21</sup> The reduction of the segregation level in sample G2/1 in comparison with G1/1 was observed because of the heterogeneity of the hard block structure, whereas the more expressed regularity in a spatial arrangement of its hard domains was caused by the reduction of  $\text{CH}_3$ -group-containing hydrazine fragments. The observed reduction of the hard domain sizes and  $D$  of their spatial alternation at the transition from G1/1 to G2/1 is connected to the decrease of the hard domain length. As the PP/DMH ratio decreased (from 2 to 20), the structural homogeneity of the hard blocks increased and promoted the increase of the  $\alpha_{\text{seg}}$  value and the decrease of the hard domain sizes in proportion to  $D$ . Thus, the newly found changes in the structure formation in DMH-based PU stipulated the structure of the macrochain and contents of allophanate, biuret, and DMH fragments and did not depend on the nature of the intermolecular physical interactions.

Figure 9 shows the results of dielectric measurements in the region of the dynamic glass transition (primary  $\alpha$ -relaxation) for some selected samples (those for SAXS measurements). On the basis of the

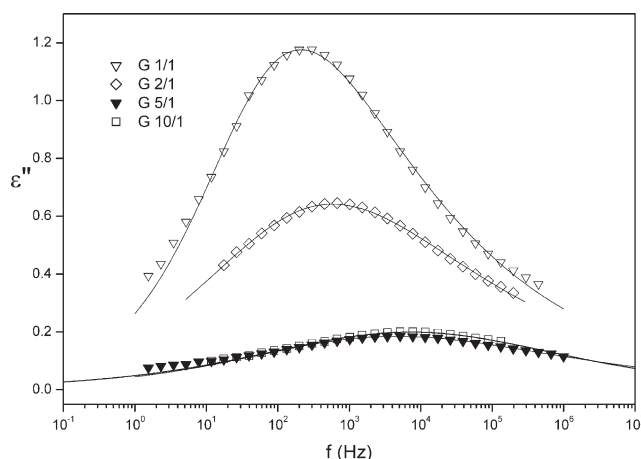


**Figure 9** Comparative  $\varepsilon''(f)$  (dependence of dielectric losses on frequency) plots at 263 K for selected PUs. The lines are fits of the Havrilia–Negami expression<sup>10</sup> to the experimental data (points).

increase of the  $\alpha_{\text{seg}}$  value with the increase of the PP/DMH ratio (from 2 to 20), one should expect that with the decrease of the DMH share, the loss peak would shift to higher frequencies, becoming larger in magnitude and narrower.<sup>22</sup> However, at the same time, the degree of branching decreases, and this should cause, similarly to networking, exactly the opposite effects. What is finally observed in Figure 9 is a compromise: the peak becomes smaller, broader, and slightly faster with the decrease of the DMH amount in the reaction mixture. Equilibrium water sorption measurements of the selected samples (used for SAXS and DRS measurements) at 25°C showed that the maximum water content (at the relative humidity of 0.98) decreased from 0.0225 for sample G1/1 to 0.0215 for sample G2/1 and to 0.0200 for sample G5/1 and increased again up to 0.0215 for sample G10/1. These results present again a compromise between the increase of the degree of microphase separation, which should cause an increase of the water uptake,<sup>22</sup> and the increase of the branching degree, which should result in a decrease of the water uptake.

## CONCLUSIONS

Novel DMH-based PUs were synthesized. The  $M_n$  values and possible structures of the PU macromolecules were proved by integrated investigations: the analysis of terminal groups by potentiometric nonaqueous titration, the determination of the nitrogen atom content according to the Kjeldal method, the aminolysis method, IR spectroscopy, viscosimetry, rheology, SAXS, DRS, and equilibrium water sorption measurements.

The reaction of PU formation proceeded via the creation of ionic reactive centers. Only in the case of a stoichiometric PP/DMH ratio (catalytic reaction) was a polymer of a linear structure and low molecular mass formed. In all other studied nonstoichiometric ratios (from 2 : 1 to 20 : 1), polymers with a branched structure (comblike) were obtained. An IR spectroscopy study of the synthesized PUs and their aminolysis products uniquely testified to the presence of the biuret (at PP/DMH = 2 : 1) and biuret and allophanate fragments (with excesses of NCO— in relation to  $\text{NH}_2$  groups of DMH by more than 4 times). These secondary bonds (biuret and allophanate) were formed in the absence of the catalyst and at a comparatively low reaction temperature (up to 80°C). The synthesized PUs displayed non-Newtonian flow and possessed thixotropic properties. The increase in the macromolecular branches lowered the polymer viscosity, except at PP/DMH = 20 : 1.

The investigation of the polymer structure by SAXS showed that the decrease of the DMH content in the reaction mixture resulted in an increase of the level of segregation. Dielectric results for the dynamic glass transition and results of water sorption measurements provided additional support for the conclusions drawn on the basis of the structural studies.

Our investigations testified to the possibility of DMH use for the formation of PUs of different structures. Effective regulation of the structure and properties of the PUs can be carried out by the simple variation of only one factor as an instrument of macromolecular design: the ratio of NCO groups of PP to  $\text{NH}_2$  groups of DMH.

## References

- Lopyrev, V. A.; Dolgushin, G. V.; Voronkov, M. G. *Zh Prikl Khim* 1998, 71, 1233 (in Russian).
- Ioffe, B. V.; Kuznetsov, M. A.; Potekhin, A. A. *Chemistry of Organic Derivatives of Hydrazine*; Khimiya: Leningrad, 1979 (in Russian).
- Savelyev, Y. V.; Grekov, A. P.; Veselov, V. Y.; Kuznetsov, S. V.; Khranovskii, V. A.; Usenko, A. A.; Kharitonova, V. K. *Ukr Khim Zh* 2000, 66, 110 (in Russian).
- Król, P. *Prog Mater Sci* 2007, 52, 915.
- Savelyer, Yu. V.; Veselov, V. Ya.; Grekov, A. P. Ukrainian Pat. 54533 (2003); Publication 17.03.2003, Bulletin No. 3 (in Ukrainian).
- Savelyev, Y. V.; Khranovskii, V. A.; Veselov, V. Y.; Grekov, A. P.; Savelyeva, O. A. *Zh Org Khim* 2003, 39, 105 (in Russian).
- Gyenes, I. In *Titration in Non-Aqueous Media*; Cohen, D.; Millar, I. T., Eds.; Academiai Kiado: Budapest, 1967.
- Bock, R. A. *Handbook of Decomposition Methods in Analytical Chemistry*; Verlag Chemie: Weinheim 1972.
- Leung, L.; Koberstein, J. T. *J. Polym Sci Polym Phys Ed* 1985, 23, 1883.
- Glatter, O.; Kratky, O. *Small-Angle X-Ray Scattering*; Academic: London, 1982.
- Laity, P.; Taylor, R.; Wang, S.; Khunkamchoo, P.; Norms, K.; Cable, M.; Andrews, G.; Johnson, A.; Cameron, R. *Polymer* 2004, 45, 7273.



12. Kripotou, S.; Pissis, P.; Bershtein, V. A.; Sysel, P.; Hobzova, R. *Polymer* 2003, 44, 2781.
13. Frank, B.; Fruebing, P.; Pissis, P. J. *Polym Sci Part B: Polym Phys* 1996, 34, 1853.
14. Grekov, A. P.; Veselov, V. Y.; Savelyev, Y. V. *Zh Org Khim* 1985, 21, 1232 (in Russian).
15. Lipatova, T. E. *Catalytic Polymerization of Oligomers and Net-Polymer Formation*; Naukova Dumka: Kiev, 1974 (in Russian).
16. Izenshtein, E. M. *Encyclopedia of Polymers*; Sovetskaya Entsiklopedia: Moscow, 1977 (in Russian).
17. Tager, A. A. *Physicokhimiya Polymerov*; Khimia: Moscow, 1978 (in Russian).
18. Lee, L. T. C.; Pearce, E. M. *J Polym Sci Part A-1: Polym Chem* 1971, 9, 557.
19. Nakanishi, K. *Infrared Absorption Spectroscopy*; Holden-Day: San Francisco, and Nankodo: Tokyo, 1962.
20. Kopusov, L. I.; Zharkov, V. V. *Plast Massy* 1972, 9 (in Russian).
21. Shtompel, V. I.; Kercha, Y. Y. *Ukr Khim Zh* 1997, 63, 53 (in Ukrainian).
22. Georgoussis, G.; Kanapitsas, A.; Pissis, P.; Savelyev, Y. V.; Veselov, V. Y.; Privalko, E. G. *Eur Polym J* 2000, 36, 1113.